



Sorption of heavy metal ions onto e-waste-derived ion-exchange material – selecting the optimum isotherm

Akanksha Kalra^a, Pejman Hadi^a, Hamish R. Mackey^b, Tareq Al Ansari^b, Gordon McKay^{a,b,*}

^aChemical and Biomolecular Engineering Department, Hong Kong University of Science and Technology, Clear Water Bay Road, Hong Kong SAR, China, Tel. +974 44541408; emails: gmckay@hbku.edu.qa (G. McKay), akanksha.kalra@manuchar.com (A. Kalra), pejman.hadimyavagh@stonybrook.edu (P. Hadi)

^bDivision of Sustainable Development, College of Science and Engineering, Hamad Bin Khalifa University, Education City, Qatar Foundation, Doha, Qatar, emails: hmackey@hbku.edu.qa (H.R. Mackey), talansari@hbku.edu.qa (T. Al Ansari)

Received 10 March 2018; Accepted 25 August 2018

ABSTRACT

This study evaluates the adsorption of metal ions, such as copper, lead and zinc, onto a silicate-based ion-exchange resin produced by activating the non-metallic fraction of printed circuit board e-waste, designated activated non-metallic-fraction printed circuit board (A-NMF-PCB), to determine the equilibrium saturation-exchange sorption capacities. The A-NMF-PCB experimental results obtained showed significant sorption-exchange capacities for copper, lead and zinc at 2.9, 3.3 and 2.1 mmol/g, respectively. These uptake values are higher than most commercial resins. The equilibrium data were analyzed using seven conventional isotherm equations, namely Langmuir, Freundlich, Langmuir–Freundlich (L–F) or Sips, Redlich–Peterson (R–P), Toth and Dubinin–Radushkevich. Five error analysis methods – sum of errors squared, hybrid error function, Marquard’s percent standard deviation, the average relative error and sum of the absolute error – were applied to each isotherm model, which were then used to obtain the best-fit model. The results demonstrated the outstanding sorption capacities of copper, lead and zinc on A-NMF-PCB. These isotherm models were then optimized by changing parameter values to get the least error value. The L–F model gave the best result for copper removal, R–P model for lead and the Toth model for zinc. The HYBRID (HYB) error function proved to be the optimum function and consequently all the isotherm models were rationalized and compared on the basis of using the HYB method. It is critical to obtain the most accurate isotherm and isotherm parameters to design sorption treatment plants.

Keywords: Error analysis; Heavy metal ions; Ion exchange; Lead; Copper; Zinc; PCB-derived waste sorbent

1. Introduction

Water pollution has become a serious concern with the increasing heavy metal pollutants contamination in freshwater bodies. Industries such as mining, microelectronics and electroplating industries discharge high levels of heavy metals into water bodies. These metals, such as chromium, arsenic, nickel, zinc, copper, etc., are potential carcinogens and pose a serious threat to human and aquatic lives. They

are non-biodegradable and accumulate in living tissues and get biomagnified through the food chain. According to government regulations, the concentration of these pollutants should be reduced to a few parts per million.

Various methods, such as coagulation–flocculation, solvent extraction, reverse osmosis and membrane separation, have been used to treat the contaminated effluents [1–4]. The main disadvantages of such methods are the associated high cost and large volume of sludge formation. Alternatively, exchange/sorption is a flexible, simple, inexpensive approach

* Corresponding author.

and insensitive to toxic materials. It can be used for toxic heavy metal-containing effluent treatment to address the concerns over high operating and capital costs, efficiency and the need for secondary treatment. Several commercial and waste-derived materials have been developed for metal ion removal in exchange/adsorption processes.

In this study, the removal of three metals, copper (Cu), lead (Pb) and zinc (Zn), by sorption/ion exchange onto an activated ion-exchange material derived from the non-metallic fraction of printed circuit board (PCB) waste is evaluated. The dangers to human health by these heavy metals have been discussed in a number of studies [5–8]. Copper is used to produce alloys such as brass or bronze, in fungicides and nutritional supplements in the form of copper sulfate. It causes many adverse effects, some of them being gastrointestinal distress, liver and kidney damage or even death in case of high levels of exposure. Lead is used in lead smelters, batteries, paper and pulp industries, boat and ship fuels, ammonium industries, in the production of television picture tubes, pigments, petroleum fuels, printing, glass industries and photographic materials. Low levels of lead can cause anemia, and high levels are capable of causing kidney dysfunction, liver, central and peripheral nervous systems and high blood pressure. Zinc is mainly used in the galvanizing industries to galvanize iron and in the preparation of alloys, as a plating material in electric batteries or in building construction for gutters. Large concentrations of zinc can affect human health and cause anemia, skin irritations or respiratory disorders among many other diseases. It also negatively affects plants and microorganisms, and only limited number of plants can survive on zinc-rich soil.

Activated carbon is traditionally the most widely used adsorbent because of its exceptionally high porosity, tunable pore size and high-adsorptive capacities [9,10]. Activated carbons have been used extensively for the removal of dyes/stuffs and organics [11], and more recently activated carbons, derived from other wastes, such as fruit stones and shells have been converted into high quality activated carbons for the removal of dyestuffs, organic compounds and metals from water [10–16]. In general, their metal ion uptake capacities are quite low and examples include the removal of lead [13,15,17,18]. Biomass-derived activated carbons are becoming popular because of the large volumes of biomass wastes available, but again their capacities for the metal ions is relatively low despite attractive purchase costs. These carbons have been used for organics [19], lead [13,17,20] and copper [12,16]. Biosorption using algal species has also been successful for the removal of copper and cadmium [21].

Several other natural materials, waste-derived materials and commercial resins have been used for the removal of heavy metals from wastewaters. For the removal of lead, these materials include peat [22], bone char [23], chickpea leaves [14] and chitosan [24]. For the removal of copper, various sorbent materials include bone char [25], peat [25], chitosan [26] and waste tyre char carbon [27]; for zinc removal, there are fewer studies reported but the materials include bone char [25,28,29] and chitosan [30]. The most widely used materials for the removal of heavy metals are ion-exchange resins, such as imminodiacetate ion-exchange resin [31] and modified carbon [29].

In this project, the sorption of copper, lead and zinc from aqueous solution onto a PCB-waste derived ion-exchange

sorbent has been studied and the capacities have been compared with other sorbents and ion exchangers. The equilibrium isotherms have been analyzed using various isotherm models, and several error analysis methods have been used to obtain the best-fit model. These error functions have been normalized across the range of all the error functions for a more accurate basis of comparison and selection of the most suitable error function which has further been used to find the most accurate isotherm constants. Determining the most correct isotherm parameters is crucial to obtaining the best design of a wastewater treatment facility in order to predict the correct removal capacity of the treatment plant.

2. Materials and experimental methodology

2.1. Materials

The PCB powder had a particle size less than 5 μm and was supplied by Total Union PCB Recycle Ltd., Lung Kwu Tan, Hong Kong. It was converted into an activated material after drying in an air oven at 378 K overnight for 24 h. We obtained the non-metallic fraction of the PCB e-waste from Total Union PCB Recycle Ltd. (Lung Kwu Tan, Hong Kong) that has developed a method for recycling electronic wastes in the form of disassembled PCBs from electronic devices, from which the components have been removed. The PCBs are mechanically comminuted in a hammermill. After the size reduction by the hammermill, the powder is separated by accelerating through a high-speed vortex with a corona electrostatic discharge producing two streams, one is a high-copper concentrate stream and the other is the non-metallic powder stream – which we used as the raw material for producing our ion-exchange sorbent, A-NMF-PCB.

Copper, zinc and lead ions were used as sorbates in this study. Copper (II), zinc (II) and lead (II) ion-bearing effluents were prepared by dissolving analytical grade hydrated copper (II) nitrate salt ($\text{Cu}(\text{NO}_3)_2 \cdot 3\text{H}_2\text{O}$), hydrated zinc (II) nitrate ($\text{Zn}(\text{NO}_3)_2 \cdot 6\text{H}_2\text{O}$) and lead (II) nitrate salt ($\text{Pb}(\text{NO}_3)_2$) with deionized (DI) water. All these salts were supplied from Sigma-Aldrich Corporation (Germany).

2.2. Methodology

2.2.1. Activation

The activation process is the enhancement of the bond cleavages, the introduction of hydroxyl group introduction and the alkali metal–hydrogen-exchange process in which not only the surface of the material, but also the inner layers are affected and exposed to the activation process, becoming available for the ion-exchange practice. The raw material precursor was impregnated in a 1 M of potassium hydroxide solution with an impregnation ratio (w/w of the precursor) of 2:1 for a 2-h period. Impregnation was carried out at room temperature and then once the impregnation was complete, the resultant solution was activated in an 18-L muffle furnace (AAF 11/18, Carbolite, UK) using an inert atmosphere.

The furnace was connected to a rotameter together with central supply of nitrogen (purity 99.99%) at the back. The furnace was controlled by a proportional-integral-derivative controller with heating rate (5°C/min) under high nitrogen

flow. To remove residual oxygen (mainly in air) in the furnace as well as gas line, the whole system was purged with nitrogen for 30 min prior to heat up. The temperature was held at 250°C for 1 h. Once the reaction was completed, the system was allowed to cool in flowing nitrogen until it reached the temperature of 110°C or below. The ceramic crucible containers were then removed from the furnace and further cooled in a desiccator.

2.2.2. Characterization

Several characterization tests have been carried out including elemental analysis, proximate analysis, heavy metal content, Brauner-Emmett-Teller (BET) nitrogen gas adsorption, X-ray fluorescence (XRF) spectrometry, X-ray photoelectron spectroscopy, particle size analysis and Fourier-transform infrared spectroscopy. The characterization results have been reported previously [32–34]. An XRF analysis of the stream was also performed. The four dominant surface materials are aluminium, silica, calcium and copper and by far the largest components are silica and calcium.

The textural properties of the sorbents were performed by determining the nitrogen adsorption/desorption isotherm at –196°C using a Quantachrome Autosorb 1. The specific surface area was calculated using the BET equation (S_{BET}). The total pore volume (V_p) was estimated from the amount of nitrogen adsorbed at a relative pressure of $P/P^\circ = 0.97$, and the average pore diameter was calculated from $D_p = 4 V_p / S_{\text{BET}}$. Pore size distribution was estimated using the Barrett, Joyner and Halenda model. The BET surface area of this sample is 240 m²/g, and we consider the activity comes from the fact that some of the potassium present in the caustic solution can be exchanged with surface hydrogen atoms rendering stronger ion-exchange properties.

2.3. Adsorption isotherm study

2.3.1. Equilibrium contact time

The equilibrium contact times for each metal were determined by contacting a constant mass of adsorbent with three metals (Cu, Zn and Pb) at a fixed concentration (1,000 ppm). For each sample, five bottles of fixed volume solutions (50 mL) with predetermined initial metal concentrations were brought into contact with fixed masses (0.05 g) of adsorbents, that is, the mass/volume ratio was 1. The bottles were sealed and agitated in the shaker bath (Gallenkamp, UK) at a speed of 120 rpm. On Day 1, 3, 5, 10 and 21 after the commencement of the run, one bottle was withdrawn from shaking. The mixtures were filtered, diluted and analyzed by inductively coupled plasma adsorption emission spectroscopy (ICP-AES). Equilibrium was achieved after 5 d.

2.3.2. Equilibrium isotherm

An accurately weighed sample (0.05 g) was added to 50 mL of single-metal solution with different initial concentrations (10–1,000 ppm). The sealed bottles were shaken at the speed of 120 rpm for 10 d in a thermostated shaker (Gallenkamp, UK) to ensure equilibrium has been reached.

The mixtures were filtered through syringe filters (0.22 μm, Millex GP, Millipore, Germany). After diluting with DI water, filtrates were analyzed by ICP-AES.

The initial concentrations of the adsorbates and the equilibrium concentrations after the equilibrium contact times were measured by ICP-AES, and the difference between them was the amount of the adsorbed metal by the adsorbent.

$$q_e = \frac{(C_0 - C_e) \times V}{m} \quad (1)$$

where C_0 and C_e are the initial and equilibrium concentrations of the metal in mmol/L, V is the volume of the solution in L, m is the mass of the adsorbent in g, and q_e is the amount of the adsorbed metal in mmol of adsorbed metal/g of adsorbent.

3. Theory

3.1. Equilibrium studies

An adsorption process reaches equilibrium when the amount of dye being adsorbed onto the adsorbent is equal to the amount being desorbed at constant temperature and pH conditions. The performance of an adsorption process can be analyzed by plotting the adsorbed dye concentration (q_e) against the equilibrium dye concentration in the liquid phase (C_e), q_e being the dependent variable. Equilibrium isotherm models are frequently used to predict or analyze the performance of adsorption processes and determine parameters such as adsorption capacity. In this study, equilibrium experiments have been conducted to find the most suitable equilibrium isotherm by evaluating and comparing errors of each isotherm and subsequently finding the optimized parameters.

3.2. Error functions

Error functions are used to evaluate how well the isotherm fits the experimental result. The choice of error function will affect the obtained isotherm parameters. Thus, we need to compare different error functions to find the function giving the least error. Error functions based on absolute deviation from original values bias the fit towards higher concentration data points. This is the case with sum of squared errors (SSE). This bias can be avoided by taking fractional deviations. However, these can bias the fit towards errors caused at lower concentration data points, which may be preferable as the greatest changes in the isotherm curve occur at these concentrations. In every isotherm case, each error function is minimized across all the concentration range studied. All the error analysis methods used in this project have been listed in Sections 3.2.1–3.2.5.

3.2.1. SSE/ERRSQ (sum of squared errors)

$$\sum (q_{e,\text{exp}} - q_{e,\text{cal}})^2 \quad (2)$$

The parameters $q_{e,\text{exp}}$ and $q_{e,\text{cal}}$ are the experimental and calculated capacities of the adsorbed material, respectively.

Eq. (2) represents the most commonly used error function, but it has a major drawback. As the magnitude of the errors and thus the squares of the errors increase, there is a biasing of the fit towards the data obtained at the high end of the concentration range. This function is available in Microsoft Solver.

3.2.2. HYB (hybrid fractional error function)

$$\sum \frac{(q_{e,\text{exp}} - q_{e,\text{cal}})^2}{q_{(e,\text{exp})}} \tag{3}$$

This error function in Eq. (3) was developed in an attempt to improve the fit of the sum of the squares of the errors at low concentrations by dividing it by the measured value [35]. The parameters n and p indicate the number of data points and number of parameters, respectively.

3.2.3. MPSD (derivative of Marquardt's percent standard deviation)

$$\sum \left[\frac{q_{e,\text{exp}} - q_{e,\text{cal}}}{q_{e,\text{exp}}} \right]^2 \tag{4}$$

This error function, Eq. (4), was used previously by a number of researchers in the field. It is similar in some respects to a geometric mean error distribution modified according to the number of degrees of freedom of the system [36].

3.2.4. ARE (average relative error)

$$\sum \left| \frac{(q_{e,\text{exp}} - q_{e,\text{cal}})}{q_{e,\text{exp}}} \right| \tag{5}$$

This error function shown in Eq. (5) attempts to minimize the fractional error distribution across the entire concentration range [37].

3.2.5. EABS (sum of absolute errors)

$$\sum |q_{e,\text{exp}} - q_{e,\text{cal}}| \tag{6}$$

This approach, represented by Eq. (6), is similar to the sum of the squares of the errors. Isotherm parameters determined using this error function would provide a better fit as the magnitude of the error increases, biasing the fit towards the high-concentration data [38].

Error analysis is performed to compare the errors of all the equilibrium isotherm models and find out which one most closely fits the experimental data – this correlation will then yield the most accurate isotherm constants.

3.3. Sum of normalized errors for isotherm selection

Each error analysis method produces errors of different magnitudes and with different biases. In order to enable a holistic assessment of the fit considering all error methods, a process of error normalization can be undertaken as described in Ho et al. [39]. In summary, the process is as follows:

1. For a given isotherm, I_i , a parameter set, $\{I_{i,k}\}$, is found by minimizing the error associated with a given error analysis method ($f_{k,\text{min}}$). This is repeated for each error method ($k = 0 \rightarrow n$) to give n different sets of parameters, where n is the number of error methods being used. This can be described as follows:

$$\{I_{i,k}\} \xrightarrow{\text{yields}} f_{k,\text{min}}(I_i) \tag{7}$$

2. For a given parameter set, $\{I_{i,k}\}$, found by minimizing a given error method, ($f_{k,\text{min}}$), there exists an associated error, $e_{i,k,\text{min},k} = f_k(\{I_{i,k}\})$. This describes the error for isotherm I found using parameters minimizing function k ($f_{k,\text{min}}$) for error analysis method k (f_k). This is repeated for each parameter set ($k = 0 \rightarrow n$) giving an $n \times n$ matrix.
3. For a given parameter set, $\{I_{i,k}\}$, the sum of normalized errors ($NE_{i,k}$) is then calculated by dividing each error for that parameter set fit by the maximum of the same error type across the other parameter sets found by minimizing different error functions, and summing these relative errors.

$$NE_{i,k} = \sum_{k=0}^n \frac{f_k(\{I_{i,k}\})}{\max_{k=0 \rightarrow n} n f_k(\{I_{i,k}\})} \tag{8}$$

4. The lowest NE for an isotherm then indicates the most suitable error analysis method for that isotherm and the best-fit parameter set.
5. Different isotherms can be compared by comparing the error produced by each isotherm model (e_i) using a selected error method. This error method is ideally the one that most frequently found the optimum parameter set/had lowest NE.

4. Results and discussion

4.1. Adsorption capacity of copper, lead and zinc metals on A-NMF-PCB

Figs. 1(a)–(c) illustrate the experimental equilibrium adsorption of three metals on A-NMF-PCB along with the best fit of each isotherm model. It can be observed that the equilibrium metal uptake (q_e) on the adsorbent increases rapidly at the beginning when the metal concentration (C_e) is low. This suggests that there are a significant number of sites available for exchange sorption, and the ion exchanger has a great affinity for the metal ions. But, as the adsorbed metal concentration increases, the adsorbent becomes saturated and the slope becomes zero. It can be seen that all three metals have similar adsorption characteristics on the A-NMF-PCB ion-exchange material. In each case, a clear maximum

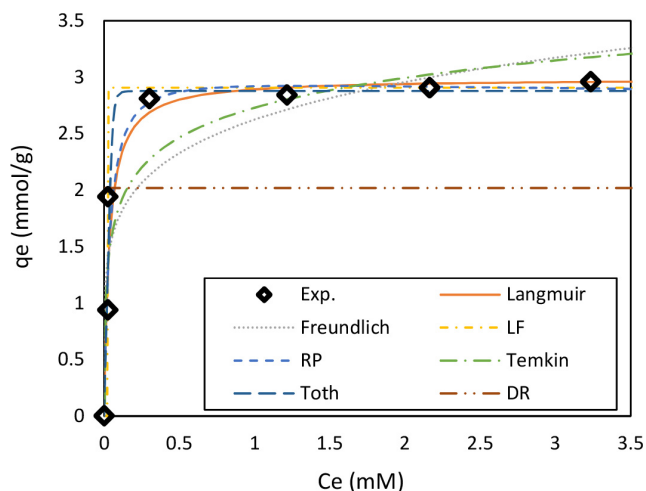


Fig. 1. Experimental data and isotherm fitting for Cu by A-NMF-PCB.

adsorption capacity was observed of 2.9 mmol/g for copper, 3.3 mmol/g for lead and 2.1 mmol/g for zinc. These values are significantly better than most studies, and comparable to the highest reported, as indicated in Table 1.

4.2. Isotherm results and discussion

For the metal systems, overall Redlich–Peterson (R–P) model, followed very closely by the Toth model gave the best result (Table 2). This was based on the average rank of each isotherm across all error methods against its peers using the fitted parameters from the NE parameter estimation. Individually, the best result for copper was obtained using the Langmuir–Freundlich (L–F) isotherm model, for zinc the R–P model and for lead the Toth model. For lead, the Toth model was also a very good fit with similar average rank as the R–P model, but was not so for copper. In general, the most commonly used Langmuir and Freundlich models did not show good fittings for the systems. It was also observed that the three parameter models usually gave better results than the two parameter models. The individual isotherms and their fittings are described subsequently.

4.2.1. Langmuir isotherm model

This model was established by Langmuir [70], and it is based on the assumptions that adsorption only takes place on a fixed number of localized sites and each site can hold only one adsorbate molecule (monolayer). In addition, all sites are identical with equal energy, and there is no interaction between adsorbed molecules. The form for a liquid state adsorption system is as follows:

$$q_e = \frac{K_L C_e}{1 + a_L C_e} = \frac{q_m a_L C_e}{1 + a_L C_e} \quad (9)$$

where C_e (mmol/L) and q_e (mmol/g) are the liquid phase metal concentrations, respectively, and K_L (L/g) and a_L (L/mmol) are Langmuir constants. The theoretical monolayer maximum capacity is represented by $q_m = K_L/a_L$. Typically when

the equilibrium equation C_e approaches zero, then Eq. (9) becomes a linear isotherm which is Henry's law as follows:

$$q_e = K_L C_e \quad (10)$$

The Langmuir constants K_L (L/g) and a_L (L/mmol) and monolayer adsorption capacities (q_0) were calculated using five error functions. These values are shown in Table 3 for the metals.

The fitting of the Langmuir isotherm for copper, lead and zinc on A-NMF-PCB is shown in Figs. 1, 2 and 3, respectively. The fit for copper and zinc was reasonable, but failed to pick up the sharp transition to the equilibrium plateau, particularly for lead.

It can be seen in Table 3 that for the data sets for copper and lead, the least error value is obtained using the HYB error function. For zinc, the least error was obtained using the EABS function, although the HYB NE was very similar (3.86 vs. 3.82). It should be noted here that the NE value only gives an indication of how consistent the error methods were at determining the respective parameters, and gives no indication against other isotherms which is the best fit of the data. For isotherm comparison, individual error analysis residuals must be compared and ranked as done in Table 2.

Moreover, we can obtain values of the constants for the best-fit isotherms using only SSE error function, ERRSQ. However, as we see in Table 4, when we perform the application of the six best-fit error functions, the analysis results in six different sets of constants can vary considerably. Thus, a rationalization of these six error functions has been carried out to compare the error functions on a common basis resulting in the best-fit overall set of the most optimum isotherm model constants using the NE approach.

The equilibrium isotherm models provide valuable information to predict exchange/sorption capacities for the design of industrial ion-exchange/sorption systems. For this reason, it is important to evaluate the isotherm parameters as accurately as possible to minimize errors in design. Table 4 presents the Langmuir constants, q_m and K_L using each of the six error analysis methods investigated in this study. In the case of q_m the differences are 3.0%, 7.5% and 2.2% for copper, lead and zinc, respectively, and for the thermodynamic parameter, K_L the differences are greater than 417%, 260% and 22% for copper, lead and zinc, respectively. The differences for the range of K_L values are very significant and could affect the design of treatment systems considerably. Therefore, it is of great importance to perform an error analysis to ensure that the most accurate isotherm is used in design and the most accurate error analysis is used to determine the best-fit isotherm constants. Corresponding tables have been generated for each isotherm for this error function analysis but only the Langmuir equation table is presented in this paper.

4.2.2. Freundlich isotherm model

The most widely used multi-site adsorption isotherm for heterogeneous surfaces is the Freundlich isotherm [71] as shown in Eq. (11):

Table 1
Adsorption capacities for copper, lead and zinc from literature and this study

Adsorbent material	Initial metal concentration (mM)	pH	Adsorbent dosage (g/L)	Adsorption capacity, q_e (mmol/g)	Reference
Copper					
Activated slag	1.57	5	20	0.47	[40]
Oxygen furnace slag	4.25	5	10	0.46	[40]
Blast furnace sludge	36.2	–	50	0.37	[41]
Fly ash	0.1–0.2	6.5	1	0.02	[42]
Red mud	1.6–9.4	5.6–6.2	1	0.31	[43]
Cellulose–chitosan composite	0.16–2.36	5	2	1.04	[44]
Garden grass	0.94–1.10	6–7	5	0.92	[45]
Peat moss	7.87	–	1	0.36	[46]
Activated carbon from cassava peel	0.063	8	10	0.13	[47]
Chemically modified orange peel	0.79–7.9	5	2	4.55	[48]
Citric acid barely straw (raw)	0.0001–0.001	6–7	1	0.5	[49]
Depectinated pomelo peel	0.39–1.97	4	5	0.33	[50]
KCl-modified orange peel	0.16–4.7	5–5.5	5	0.94	[51]
Mango peel waste	0.16–7.9	5–6	5	0.73	[52]
Mg ²⁺ -modified orange peel	0.16–4.7	5–5.5	5	0.64	[53]
Pomelo peel	0.39–1.97	4	5	0.31	[50]
Sunflower hull (raw)	0.39–7.9	5	2	0.9	[54]
Sewage sludge carbons	1.57	5	0.5	1.31	[55]
Cancrinite-type zeolite from fly ash	0.5–4	6	0.5	2.08	[56]
A-NMF-PCB	3.1	–	1	2.9	This study
Lead					
Agave bagasse (raw)	0.29	5	2	0.17	[57]
Agave bagasse (HCl)	0.29	5	1	0.20	[57]
Agave bagasse (HNO ₃)	0.29	5	1	0.13	[57]
Agave bagasse (NaOH)	0.29	5	1	0.24	[57]
KCl-modified orange peel	0.05–1.45	5–5.5	5	0.68	[51]
Sulfured orange peel	0.12–3.9	5	5	0.79	[58]
Orange peel xanthate (XOP)	0.48	–	5	1.05	[59]
Mercerized garlic peel	0.005–0.97	5	0.5	0.53	[60]
Native garlic peel	0.005–0.97	5	0.5	0.25	[60]
Lentil husk	0.24	5	2	0.39	[61]
Ponkan peel	15	5	2	0.54	[62]
Peat moss	2.41	–	1	0.19	[46]
<i>Sargassum</i> sp. (algae)	0.05–0.72	2–7	4	1.28	[63]
Seaweed	–	5.5	–	1.78	[64]
Activated carbon from cassava peel	0.08	8	10	0.03	[47]
Muskmelon peel	1–5	4.5	5	0.81	[65]
Black liquor	0.01–0.1	4–6	2–6	0.09	[66]
Blast furnace sludge	24.1	–	50	0.39	[41]
Red mud	2.41–4.83	4	10	0.31	[67]
Cancrinite-type zeolite from fly ash	0.5–4	6	0.5	2.53	[56]
Natural zeolite	8.94	5.2	10	1.71	[68]
A-NMF-PCB	3.38	–	1	3.3	This study
Zinc					
Agave bagasse (raw)	0.92	5	2	0.12	[57]
Agave bagasse (HCl)	0.92	5	1	0.19	[57]
Agave bagasse (HNO ₃)	0.92	5	1	0.22	[57]
Agave bagasse (NaOH)	0.92	5	1	0.31	[57]
KCl-modified orange peel	0.05–1.45	5–5.5	5	0.71	[51]
Sulfured orange peel	0.38–12.2	5	5	1.22	[58]
XOP	0.76	–	5	0.76	[59]
Raw <i>Eucalyptus sheathiana</i> bark	0.31–1.07	5	0.25	1.96	[69]
NaOH-treated <i>E. sheathiana</i> bark	0.31–1.07	5	0.25	3.82	[69]
D401 chelating resin	–	–	–	2.1	[31]
Natural zeolite tuff	0.57–10.08	5.3–5.5	–	0.20	[68]
Black liquor	0.01–0.1	4–6	2–6	1.45	[66]
Blast furnace slag	1.52	6	20	0.27	[40]
Red mud	3.05–10.7	6.9–7.8	1	0.19	[43]
Cancrinite-type zeolite from fly ash	0.5–4.0	6	0.5	1.53	[56]
A-NMF-PCB	3.38	–	1	2.1	This study

Table 2

Ranked fit of the different isotherm models based on average rank across the five different error analysis methods for the most optimal parameter fit found using the normalized error approach

	Langmuir	Freundlich	L-F	R-P	Temkin	Toth	D-R
Cu	3.4	6	1	2.2	4.8	3.6	7
Pb	2.8	5.4	5	1.6	4.4	1.8	7
Zn	2.6	5	6.6	2.2	4	1.2	6.4
Average	2.9	5.5	4.2	2	4.4	2.2	6.8

Table 3

Isotherm constants with least error analysis details for each of the three metals

Parameter	1	2	3	Least error method	Least normalized error value
Langmuir	K_L (L/g)	a_L (L/mmol)	q_0 (mmol/g)		
Cu	29.707	9.939	2.989	HYB	2.711
Pb	42.65	12.59	3.388	HYB	3.122
Zn	8.658	3.970	2.181	EABS	3.817
Freundlich	K_F (L/g)	b_F	–		
Cu	2.624	0.1728	–	HYB	3.059
Pb	2.979	0.1381	–	HYB	3.872
Zn	1.763	0.2257	–	HYB	3.516
Sips	q_m (mmol/g)	K_{L-F} (L/mmol)	$1/n_{L-F}$		
Cu	2.907	2.92E + 88	55.28	EABS	3.320
Pb	3.249	2.55E + 74	44.67	MPSD	3.932
Zn	1.768	3.41E + 78	49.07	ERRSQ	3.303
R-P	K_R (L/g)	a_R (L/mmol)	B		
Cu	81.56	26.93	1.027	HYB	4.247
Pb	86.33	22.54	1.221	HYB	3.932
Zn	15.29	6.538	1.068	MPSD	3.388
Temkin	K_t (L/g)	α	–		
Cu	1,283	0.3813	–	HYB	3.602
Pb	5,013	0.3618	–	HYB	3.386
Zn	152.6	0.3674	–	MPSD	3.935
Toth	K_T (mmol/g)	β	α_T (mmol ^{β} /L ^{β})		
Cu	2.877	5.303	2.396E – 7	HYB	3.544
Pb	3.313	4.206	3.959E – 6	MPSD	2.429
Zn	2.082	1.560	0.0592	MPSD	3.935
D-R	q_D	B_D	–		
Cu	2.019	0	–	HYB	3.140
Pb	2.317	0	–	HYB	3.180
Zn	1.768	0	–	ERRSQ	3.303

$$q_e = K_F C_e^{b_F} \quad (11)$$

where K_F is a constant related to the adsorption capacity and b_F is a constant related to the surface heterogeneity where values close to 1 indicate more homogenous adsorption. The equation was derived by assuming an exponential decay energy distribution function. The Freundlich model is widely applied in heterogeneous systems, especially for the adsorption of organic compounds. Contrary to the Langmuir model, it does not obey Henry's law at low concentrations. The amount of adsorbed material is the summation of all adsorbed sites.

The Freundlich isotherm model in Eq. (11) is often used to describe adsorption processes on activated carbon and also metal exchange/sorption. The Freundlich constant K_F (L/g) and heterogeneity factor b_F are calculated and shown in Table 3 for the three metal systems. The Freundlich constant is an empirical constant depending on several environmental factors. The factor b_F ranges between 0 and 1. It indicates the degree of non-linearity between solution concentration and adsorption. If the value of b_F is equal to unity, the adsorption is linear, which means the q_e value is proportional to C_e value; if the value is below unity, the adsorption process is chemical like the metal ion exchange in this study; if the value is above unity, the adsorption is more likely to be a physical

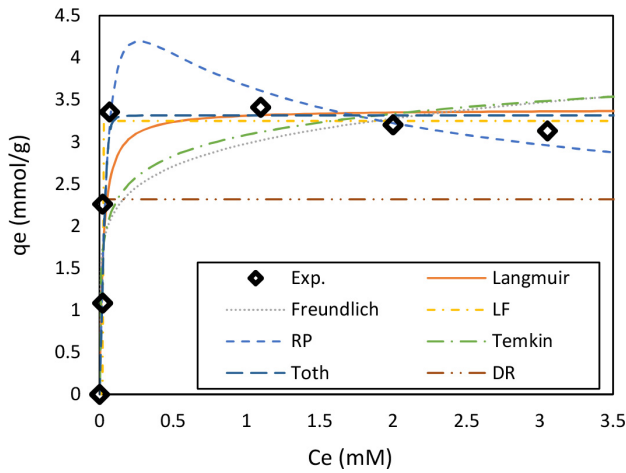


Fig. 2. Experimental data and isotherm fitting for Pb by A-NMF-PCB.

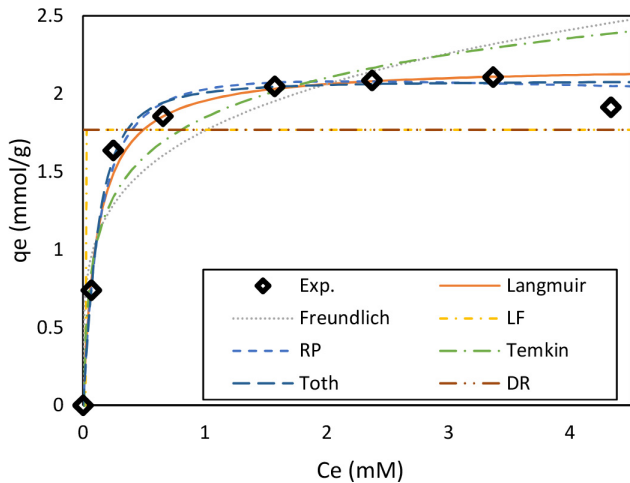


Fig. 3. Experimental data and isotherm fitting for Zn by A-NMF-PCB.

Table 4
Comparison of Langmuir isotherm parameters derived using minimization of different error methods

		ERRSQ	HYB	MPSD	ARE	EABS
Cu	q_m	2.967	2.989	3.012	2.979	2.924
	K_L	38.03	29.71	24.25	18.53	77.42
Pb	q_m	3.373	3.388	3.397	3.274	3.159
	K_L	60.20	42.65	32.23	23.12	34.03
Zn	q_m	2.192	2.211	2.229	2.214	2.181
	K_L	9.062	8.339	7.828	7.441	8.658

process. A value b_f closer to zero indicates a more heterogeneous surface.

The Freundlich fit was poor for all three metals (Figs. 1–3), notably because the Freundlich does not plateau to a maximum capacity while the experimental data showed a very rapid and distinct plateau. For copper and lead, the least error value was using the HYB function, while for zinc the HYB was second best, bettered by the MPSD function.

4.2.3. Sips (L–F) isotherm model

The Sips isotherm is derived by combining the Langmuir and the Freundlich expressions, hence also deriving the name L–F isotherm [72]. It is used to predict heterogeneous adsorption systems.

$$q_e = \frac{q_m \cdot K_{LF} \cdot C_e^{\frac{1}{n_{LF}}}}{1 + K_{LF} \cdot C_e^{\frac{1}{n_{LF}}}} \quad (12)$$

where q_m is a parameter related to the adsorption capacity, K_{LF} is a constant related to the energy of adsorption and n_{LF} is an exponent related to the heterogeneity. At low metal ion concentrations, Eq. (12) reduces to the Freundlich equation and does not obey Henry’s law. When $n_{LF} = 1$, the equation approaches the Langmuir equation. The isotherm constants for the L–F model are shown in Table 3 and are plotted in Figs. 1–3.

In the case of the L–F model, the most suitable error method varied for each metal: EABS for copper, MPSD for lead (although both ARE and EABS provided very similar NE) and ERSSQ for zinc sorption (although the HYB was very close for zinc). Such differences are due to the degree of curvature in the experimental isotherm curve and the way these error methods handle error in the mid-range of the curve. For lead, it shows the greatest curvature and therefore the L–F model showed the greatest deviations in the mid-concentration range of the curve where the balanced approach of the HYB function accounts for these variations best. The L–F was the optimal isotherm for copper, and was the only metal where an isotherm was confirmed by all error methods as the best. However, it was a poor fit for both lead and zinc (Table 2).

4.2.4. R–P isotherm model

The R–P isotherm is a hybrid isotherm encompassing the features of both the Langmuir and Freundlich isotherms and does not follow the restriction of monolayer sorption [73].

$$q_e = \frac{K_R C_e}{1 + a_R C_e^\beta} \quad (13)$$

It is an empirical equation with three parameters, K_R (L/g), a_R (L/mmol) and β . The exponent β lies between 0 and 1. When $\beta = 1$, the equation is equal to the Langmuir equation; when $\beta = 0$, it becomes Henry’s law.

The R–P curve fittings were relatively strong across all metals, such that overall R–P was the most suitable isotherm, as well as for lead. The β values close to 1 for copper and less so for zinc, which indicate the curves are almost the same as the Langmuir isotherm. This was not the case with lead. The least error value for copper and lead is obtained using the HYB analysis, whereas MPSD gives the lowest value for zinc. The β values, all relatively close to unity, can also be explained by the fact that the experimental q_e values become almost constant at the monolayer corresponding to maximum exchange sorption as in the Langmuir isotherm.

4.2.5. Temkin isotherm model

The Temkin isotherm is an early model describing the adsorption of hydrogen onto platinum electrodes within the acidic solutions. This model is excellent and has been widely used for describing gas adsorption. An assumption is made that heat of adsorption (function of temperature) of all molecules in the layer would decrease linearly rather than logarithmically with surface coverage [74].

$$q_e = \alpha \ln(K_T C_e) = \frac{RT}{b} \ln(K_T C_e) \quad (14)$$

where α is a constant related to heat of adsorption (J/mol), K_T is the Temkin isotherm equilibrium binding constant (L/g), R is the universal gas constant (8.314 J/mol/K), T is the temperature (°K) and b is the Temkin isotherm constant.

For the Temkin isotherm, the optimum error analysis method was the HYB method for all three metals. The model values were consistently low in the transition region of the isotherm curve and high in the plateau region for all metals describing a poor fit where the residual errors are not randomly distributed. The overall fit comparison with other isotherms (Table 2) indicates the Temkin model is a relatively poor fit to the data for all three metals.

4.2.6. Toth isotherm model

The Toth isotherm is derived from potential theory and is applicable to heterogeneous adsorption. According to the theory, there is a quasi-Gaussian energy distribution. The energy levels of most adsorption sites are lower than the peak or maximum adsorption energy [75]. It obeys Henry's law at low concentration. The Toth isotherm equation has the following form:

$$q_e = \frac{K_T C_e}{(\alpha_T + C_e^\beta)^{\frac{1}{\beta}}} \quad (15)$$

where K_T is a parameter related to the maximum adsorption capacity (mol/g), α_T is a Toth saturation constant (mol^β/L^β) and β is a heterogeneity coefficient, which takes a value of 0 to 1. At $\beta = 1$ the Toth isotherm tends more towards the Langmuir isotherm.

For the copper sorption system, the HYB error method gave the optimum parameter set, while MPSD was the optimum error method for both lead and zinc. The Toth constants are listed in Table 3, and the isotherm fitting shown in Figs. 1–3 which is amongst the best of the isotherms. Overall the Toth isotherm was the second best-fitting isotherm, close behind the R–P isotherm and was clearly best for zinc.

4.2.7. D–R isotherm model

The Dubinin–Radushkevich (D–R) equation was proposed as an empirical adaptation of the Polanyi adsorption potential theory. Because it has been the fundamental equation to quantitatively describe the gas adsorption and vapour adsorption by microporous adsorbents [76]. The mechanism

for adsorption in the micropores is that of pore-filling rather than layer-by-layer surface coverage.

$$q_e = q_m e^{B_D \left(RT \ln \left(1 + \frac{1}{C_e} \right) \right)^2} \quad (16)$$

where q_m is a constant related to the maximum adsorption capacity and B_D is a parameter related to the inverse of the energy of adsorption squared.

The HYB method gave the optimal parameters for copper and lead, while ERRSQ was the optimal error method for zinc. These two error methods and ARE were all close. The D–R isotherm was not suitable for the studied sorption system, receiving the worst ranking for errors across all error methods for copper and lead, and except for three error methods where the D–R isotherm outperformed the L–F isotherm, was also the worst for zinc. Furthermore, the D–R showed a consistent pattern of underestimating the maximum equilibrium capacity while overestimating the equilibrium capacity at low equilibrium concentrations (Figs. 1–3).

4.3. Error analysis

4.3.1. Best error function

In Table 4, the normalized error functions having the lowest values for the corresponding isotherm models and metal are summarized. The HYB error method gives the best results for 13 out of 24 of the systems followed by MPSD which gives best results for 4 systems. EABS and ERRSQ both give the optimum data set for two systems. Thus, HYB error analysis function can be considered from this study as the most robust error analysis method if one were to choose only one optimization function. This is in comparison to ERRSQ which is the most commonly used error function which performed relatively poorly. The more representative and stronger performance of the HYB model can be considered due to its form balancing the influence of relative and absolute errors in the fit. When only absolute errors are considered the fit tends to favour fitting to data points at lower values of the independent variable, while relative errors tend to favour data points associated with larger values of the independent variable. The HYB results will be used for further comparison of isotherm models for metals data.

4.3.2. Best-fit model

From the previous tables (Tables 3 and 5), we obtain the HYB as the best error function. Thus, we compared the error values of all the isotherms for each metal ion system using HYB error values. The isotherm giving the least error value is listed in the following Table 6 for all the three metal systems. The error values were compared using the absolute values of the HYB function, as this was the best error function as obtained from Table 4. These results are similar to those in Table 1 that were determined found using a ranking across all error methods, showing that the HYB error function alone is a suitable and reliable method for optimization and error minimization.

Among the three sorption systems, the TOOTH gave the best prediction as it gave the best and second best fits for

Table 5

Composite table for normalized errors showing the least values for the three metals

	Cu	Pb	Zn
Langmuir	2.711 (HYB)	3.122 (HYB)	3.817 (EABS)
Freundlich	3.059 (HYB)	3.872 (HYB)	3.516 (HYB)
Sips	3.320 (EABS)	3.272 (MPSD)	3.303 (ERRSQ)
R–P	4.247 (HYB)	3.932 (HYB)	3.388 (MPSD)
Temkin	3.602 (HYB)	3.386 (HYB)	3.936 (HYB)
Toth	3.544 (HYB)	2.429 (MPSD)	3.935 (MPSD)
D–R	3.140 (HYB)	3.180 (HYB)	3.303 (ERRSQ)

Table 6

Best-fit model for different sorption isotherms for metals based on HYB error function

A-NMF-PCB	Best-fit model	HYB
Cu	L–F	0.00775
Pb	R–P	0.4844
Zn	Toth	0.00623
Combined	Toth	0.2776

two systems; and had the lowest average absolute residual across the three metals, although the value for the R–P was extremely close (0.2784). Similar to Table 2, the Toth model was a close contender for the best-fit isotherm to lead data with an absolute error of 0.4941. Different parameter sets and different optimum isotherms (see Table 2) can result from fitting isotherms using different error functions. As these results show, the optimum is not frequently found using the standard ERRSQ error function. Thus, error analysis needs to be carried out in order to find the most optimum isotherm model and in particular the best fit isotherm constants to enable the optimum treatment system to be designed.

5. Conclusions

The equilibrium isotherms have been measured for three metal ions, namely, copper, lead and zinc, onto a novel ion exchanger derived from the non-metallic aluminosilicate component of PCB e-waste. The metal uptake capacities were exceptionally high compared with many commercial ion-exchange materials. The equilibrium data were analyzed by several isotherms and the errors in each isotherm were assessed using five classical error functions. The errors which were then normalized so that they could be compared with each other and the best isotherm model with the best error function could be identified. The Toth and R–P isotherms provided the least NE value overall for all the three metal ions on A-NMF-PCB systems, and the isotherm curves also fit well to the experimental data. The importance of the research enables the best-fit isotherm to be selected to predict the correct capacity of a wastewater treatment plant during the process design phase. The HYB error function was a clear leader in terms of reducing overall error and is recommended as a preferred optimization function over the more widely used ERRSQ.

References

- [1] G.P. Broom, R.C. Squires, M.P.J. Simpson, I. Martin, The treatment of heavy metal effluents by crossflow microfiltration, *J. Membr. Sci.*, 87 (1994) 219–230.
- [2] M.M. Matlock, B.S. Howerton, D.A. Atwood, Chemical precipitation of lead from lead battery recycling plant wastewater, *Ind. Eng. Chem. Res.*, 41 (2002) 1579–1582.
- [3] G. Mezohegyi, F.P. van der Zee, J. Font, A. Fortuny, A. Fabregat, Towards advanced aqueous dye removal processes: a short review on the versatile role of activated carbon, *J. Environ. Manage.*, 102 (2012) 148–164.
- [4] T. Robinson, G. McMullan, R. Marchant, P. Nigam, Remediation of dyes in textile effluent: a critical review on current treatment technologies with a proposed alternative, *Bioresour. Technol.*, 77 (2001) 247–255.
- [5] US EPA, National Primary Drinking Water Regulation, U.S. Environmental Protection Agency, 2009.
- [6] M.A. Shannon, P.W. Bohn, M. Elimelech, J.G. Georgiadis, B.J. Mariñas, A.M. Mayes, Science and technology for water purification in the coming decades, *Nature*, 452 (2008) 301.
- [7] B.R. Stern, M. Solioz, D. Krewski, P. Aggett, T.C. Aw, S. Baker, K. Crump, M. Dourson, L. Haber, R. Hertzberg, C. Keen, B. Meek, L. Rudenko, R. Schoeny, W. Slob, T. Starr, Copper and human health: biochemistry, genetics, and strategies for modeling dose-response relationships, *J. Toxicol. Environ. Health Part B*, 10 (2007) 157–222.
- [8] N. Ünlü, M. Ersoz, Adsorption characteristics of heavy metal ions onto a low cost biopolymeric sorbent from aqueous solutions, *J. Hazard. Mater.*, 136 (2006) 272–280.
- [9] P. Hadi, K.Y. Yeung, J. Barford, K.J. An, G. McKay, Significance of “effective” surface area of activated carbons on elucidating the adsorption mechanism of large dye molecules, *J. Environ. Chem. Eng.*, 3 (2015) 1029–1037.
- [10] B.H. Hameed, I.A.W. Tan, A.L. Ahmad, Adsorption isotherm, kinetic modeling and mechanism of 2,4,6-trichlorophenol on coconut husk-based activated carbon, *Chem. Eng. J.*, 144 (2008) 235–244.
- [11] M. Valix, W.H. Cheung, G. McKay, Preparation of activated carbon using low temperature carbonisation and physical activation of high ash raw bagasse for acid dye adsorption, *Chemosphere*, 56 (2004) 493–501.
- [12] Y. Li, B. Zhao, L. Zhang, R. Han, Biosorption of copper ion by natural and modified wheat straw in fixed-bed column, *Desal. Wat. Treat.*, 51 (2013) 5735–5745.
- [13] L. Mouni, L. Belkhir, F. Zougaghe, M. Tafer, Removal of Pb(II) from aqueous solution by adsorption using activated carbon developed from *Apricot* stone: equilibrium and kinetic, *Desal. Wat. Treat.*, 52 (2014) 6412–6419.
- [14] M. Nadeem, I.B. Tan, M.R.U. Haq, S.A. Shahid, S.S. Shah, G. McKay, Sorption of lead ions from aqueous solution by chickpea leaves, stems and fruit peelings, *Adsorpt. Sci. Technol.*, 24 (2006) 269–282.
- [15] G.E. Sharaf El-Deen, S.E.A. Sharaf El-Deen, Kinetic and isotherm studies for adsorption of Pb(II) from aqueous solution onto coconut shell activated carbon, *Desal. Wat. Treat.*, 57 (2016) 28910–28931.
- [16] J. Shou, M. Qiu, Adsorption of copper ions onto activated carbon from capsicum straw, *Desal. Wat. Treat.*, 57 (2016) 353–359.
- [17] L. Mouni, D. Merabet, A. Bouzaza, L. Belkhir, Removal of Pb²⁺ and Zn²⁺ from the aqueous solutions by activated carbon prepared from *Dates stone*, *Desal. Wat. Treat.*, 16 (2010) 66–73.
- [18] M. Nadeem, A. Mahmood, S.A. Shahid, S.S. Shah, A.M. Khalid, G. McKay, Sorption of lead from aqueous solution by chemically modified carbon adsorbents, *J. Hazard. Mater.*, 138 (2006) 604–613.
- [19] E.L.K. Mui, W.H. Cheung, M. Valix, G. McKay, Dye adsorption onto char from bamboo, *J. Hazard. Mater.*, 177 (2010) 1001–1005.
- [20] Q.-S. Liu, Properties of chemically prepared corncob-based activated carbons and their adsorption characteristics for aqueous lead and phenol, *Desal. Wat. Treat.*, 72 (2017) 197–206.
- [21] K. Kipigroch, M. Janosz-Rajczyk, R. Mosakowska, Sorption of copper (II) and cadmium (II) ions with the use of algae, *Desal. Wat. Treat.*, 52 (2014) 3987–3992.

- [22] Y.S. Ho, G. McKay, Kinetic model for lead(II) sorption on peat, *Adsorpt. Sci. Technol.*, 16 (1998) 243–255.
- [23] D.C.K. Ko, J.F. Porter, G. McKay, Optimised correlations for the fixed-bed adsorption of metal ions on bone char, *Chem. Eng. Sci.*, 55 (2000) 5819–5829.
- [24] J.C.Y. Ng, W.H. Cheung, G. McKay, Equilibrium studies for the sorption of lead from effluents using chitosan, *Chemosphere*, 52 (2003) 1021–1030.
- [25] C.W. Cheung, J.F. Porter, G. McKay, Removal of Cu(II) and Zn(II) ions by sorption onto bone char using batch agitation, *Langmuir*, 18 (2002) 650–656.
- [26] J.C.Y. Ng, W.H. Cheung, G. McKay, Equilibrium studies of the sorption of Cu(II) ions onto chitosan, *J. Colloid Interface Sci.*, 255 (2002) 64–74.
- [27] A. Shahtalebi, M.H. Sarrafzadeh, G. McKay, An adsorption diffusion model for removal of copper (II) from aqueous solution by pyrolytic tyre char, *Desal. Wat. Treat.*, 51 (2013) 5664–5673.
- [28] J. Moreno-Pérez, A. Bonilla-Petriciolet, C.K. Rojas-Mayorga, D.I. Mendoza-Castillo, M. Mascia, M. Errico, Adsorption of zinc ions on bone char using helical coil-packed bed columns and its mass transfer modeling, *Desal. Wat. Treat.*, 57 (2016) 24200–24209.
- [29] L. Pivarčiová, O. Rosskopfová, M. Galamboš, P. Rajec, Adsorption behavior of Zn(II) ions on synthetic hydroxyapatite, *Desal. Wat. Treat.*, 55 (2015) 1825–1831.
- [30] V.-P. Dinh, N.-C. Le, V.-D. Nguyen, N.-T. Nguyen, Adsorption of zinc (II) onto MnO₂/chitosan composite: equilibrium and kinetic studies, *Desal. Wat. Treat.*, 58 (2017) 427–434.
- [31] T.-H. Shek, A. Ma, V.K.C. Lee, G. McKay, Kinetics of zinc ions removal from effluents using ion exchange resin, *Chem. Eng. J.*, 146 (2009) 63–70.
- [32] P. Hadi, J. Barford, G. McKay, Toxic heavy metal capture using a novel electronic waste-based material—mechanism, modeling and comparison, *Environ. Sci. Technol.*, 47 (2013) 8248–8255.
- [33] P. Hadi, M. Xu, C.S.K. Lin, C.-W. Hui, G. McKay, Waste printed circuit board recycling techniques and product utilization, *J. Hazard. Mater.*, 283 (2015) 234–243.
- [34] M. Xu, P. Hadi, C. Ning, J. Barford, K.J. An, G. McKay, Aluminosilicate-based adsorbent in equimolar and non-equimolar binary-component heavy metal removal systems, *Water Sci. Technol.*, 72 (2015) 2166–2178.
- [35] S.J. Allen, G. McKay, J.F. Porter, Adsorption isotherm models for basic dye adsorption by peat in single and binary component systems, *J. Colloid Interface Sci.*, 280 (2004) 322–333.
- [36] D.W. Marquardt, An algorithm for least-squares estimation of nonlinear parameters, *J. Soc. Ind. Appl. Math.*, 11 (1963) 431–441.
- [37] J.F. Porter, G. McKay, K.H. Choy, The prediction of sorption from a binary mixture of acidic dyes using single- and mixed-isotherm variants of the ideal adsorbed solute theory, *Chem. Eng. Sci.*, 54 (1999) 5863–5885.
- [38] G. McKay, A. Mesdaghinia, S. Nasser, M. Hadi, M. Solaimany Aminabad, Optimum isotherms of dyes sorption by activated carbon: fractional theoretical capacity & error analysis, *Chem. Eng. J.*, 251 (2014) 236–247.
- [39] Y.S. Ho, J.F. Porter, G. McKay, Equilibrium isotherm studies for the sorption of divalent metal ions onto peat: copper, nickel and lead single component systems, *Water Air Soil Pollut.*, 141 (2002) 1–33.
- [40] V.K. Gupta, Equilibrium uptake, sorption dynamics, process development, and column operations for the removal of copper and nickel from aqueous solution and wastewater using activated slag, a low-cost adsorbent, *Ind. Eng. Chem. Res.*, 37 (1998) 192–202.
- [41] A. López-Delgado, C. Pérez, F.A. López, Sorption of heavy metals on blast furnace sludge, *Water Res.*, 32 (1998) 989–996.
- [42] K.K. Panday, G. Prasad, V.N. Singh, Copper (II) removal from aqueous solutions by fly ash, *Water Res.*, 19 (1985) 869–873.
- [43] E. López, B. Soto, M. Arias, A. Núñez, D. Rubinos, M.T. Barral, Adsorbent properties of red mud and its use for wastewater treatment, *Water Res.*, 32 (1998) 1314–1322.
- [44] S. Peng, H. Meng, Y. Ouyang, J. Chang, Nanoporous magnetic cellulose–chitosan composite microspheres: preparation, characterization, and application for Cu(II) adsorption, *Ind. Eng. Chem. Res.*, 53 (2014) 2106–2113.
- [45] M.A. Hossain, H.H. Ngo, W.S. Guo, T. Setiadi, Adsorption and desorption of copper(II) ions onto garden grass, *Bioresour. Technol.*, 121 (2012) 386–395.
- [46] J.K. McLellan, C.A. Rock, Pretreating landfill leachate with peat to remove metals, *Water Air Soil Pollut.*, 37 (1988) 203–215.
- [47] H.I. Owamah, Biosorptive removal of Pb(II) and Cu(II) from wastewater using activated carbon from cassava peels, *J. Mater. Cycles Waste Manage.*, 16 (2014) 347–358.
- [48] N. Feng, X. Guo, S. Liang, Adsorption study of copper (II) by chemically modified orange peel, *J. Hazard. Mater.*, 164 (2009) 1286–1292.
- [49] E. Pehlivan, T. Altun, Ş. Parlayici, Modified barley straw as a potential biosorbent for removal of copper ions from aqueous solution, *Food Chem.*, 135 (2012) 2229–2234.
- [50] P. Tasaso, Adsorption of copper using pomelo peel and depectinated pomelo peel, *J. Clean Energy Technol.*, 2 (2014) 154–157.
- [51] Z. Cao, Y. He, L. Sun, X. Cao, Removal of heavy metal ions from aqueous solutions by adsorption using modified orange peel as adsorbent, *Adv. Mater. Res.*, 236–238 (2011) 237–240.
- [52] M. Iqbal, A. Saeed, I. Kalim, Characterization of adsorptive capacity and investigation of mechanism of Cu²⁺, Ni²⁺ and Zn²⁺ adsorption on mango peel waste from constituted metal solution and genuine electroplating effluent, *Sep. Sci. Technol.*, 44 (2009) 3770–3791.
- [53] S. Liang, X. Guo, N. Feng, Q. Tian, Isotherms, kinetics and thermodynamic studies of adsorption of Cu²⁺ from aqueous solutions by Mg²⁺/K⁺ type orange peel adsorbents, *J. Hazard. Mater.*, 174 (2010) 756–762.
- [54] A. Witek-Krowiak, Analysis of temperature-dependent biosorption of Cu²⁺ ions on sunflower hulls: kinetics, equilibrium and mechanism of the process, *Chem. Eng. J.*, 192 (2012) 13–20.
- [55] S. Rio, C. Faur-Brasquet, L.L. Coq, P. Courcoux, P.L. Cloirec, Experimental design methodology for the preparation of carbonaceous sorbents from sewage sludge by chemical activation—application to air and water treatments, *Chemosphere*, 58 (2005) 423–437.
- [56] W. Qiu, Y. Zheng, Removal of lead, copper, nickel, cobalt, and zinc from water by a cancrinite-type zeolite synthesized from fly ash, *Chem. Eng. J.*, 145 (2009) 483–488.
- [57] L.H. Velazquez-Jimenez, A. Pavlick, J.R. Rangel-Mendez, Chemical characterization of raw and treated agave bagasse and its potential as adsorbent of metal cations from water, *Ind. Crops Prod.*, 43 (2013) 200–206.
- [58] S. Liang, X. Guo, Q. Tian, Adsorption of Pb²⁺ and Zn²⁺ from aqueous solutions by sulfured orange peel, *Desalination*, 275 (2011) 212–216.
- [59] S. Liang, X.-y. Guo, N.-c. Feng, Q.-h. Tian, Effective removal of heavy metals from aqueous solutions by orange peel xanthate, *Trans. Nonferrous Met. Soc. China*, 20 (2010) s187–s191.
- [60] W. Liu, Y. Liu, Y. Tao, Y. Yu, H. Jiang, H. Lian, Comparative study of adsorption of Pb(II) on native garlic peel and mercerized garlic peel, *Environ. Sci. Pollut. Res.*, 21 (2014) 2054–2063.
- [61] M. Basu, A.K. Guha, L. Ray, Biosorptive removal of lead by lentil husk, *J. Environ. Chem. Eng.*, 3 (2015) 1088–1095.
- [62] F.A. Pavan, A.C. Mazzocato, R.A. Jacques, S.L.P. Dias, Ponkan peel: a potential biosorbent for removal of Pb(II) ions from aqueous solution, *Biochem. Eng. J.*, 40 (2008) 357–362.
- [63] B.L. Martins, C.C.V. Cruz, A.S. Luna, C.A. Henriques, Sorption and desorption of Pb²⁺ ions by dead *Sargassum* sp. biomass, *Biochem. Eng. J.*, 27 (2006) 310–314.
- [64] S. Ahmady-Asbchin, Y. Andres, C. Gerente, P.L. Cloirec, Natural seaweed waste as sorbent for heavy metal removal from solution, *Environ. Technol.*, 30 (2009) 755–762.
- [65] K. Huang, H. Zhu, Removal of Pb²⁺ from aqueous solution by adsorption on chemically modified muskmelon peel, *Environ. Sci. Pollut. Res.*, 20 (2013) 4424–4434.
- [66] S.K. Srivastava, A.K. Singh, A. Sharma, Studies on the uptake of lead and zinc by lignin obtained from black liquor – a paper industry waste material, *Environ. Technol.*, 15 (1994) 353–361.

- [67] V.K. Gupta, M. Gupta, S. Sharma, Process development for the removal of lead and chromium from aqueous solutions using red mud—an aluminium industry waste, *Water Res.*, 35 (2001) 1125–1134.
- [68] J. Perić, M. Trgo, N. Vukojević Medvidović, Removal of zinc, copper and lead by natural zeolite—a comparison of adsorption isotherms, *Water Res.*, 38 (2004) 1893–1899.
- [69] S. Afroze, T.K. Sen, H.M. Ang, Adsorption removal of zinc (II) from aqueous phase by raw and base modified *Eucalyptus sheathiana* bark: kinetics, mechanism and equilibrium study, *Process Saf. Environ. Prot.*, 102 (2016) 336–352.
- [70] I. Langmuir, The adsorption of gases on plane surfaces of glass, mica and platinum, *J. Am. Chem. Soc.*, 40 (1918) 1361–1403.
- [71] H.M.F. Freundlich, Over the adsorption in solution, *J. Phys. Chem.*, 57 (1906) 385–471.
- [72] R. Sips, On the structure of a catalyst surface, *J. Chem. Phys.*, 16 (1948) 490–495.
- [73] O. Redlich, D.L. Peterson, A useful adsorption isotherm, *J. Phys. Chem.*, 63 (1959) 1024.
- [74] M. Temkin, V. Pyzhev, Kinetics of ammonia synthesis on promoted iron catalysts, *Acta Physiochim. URSS*, 12 (1940) 217–222.
- [75] J. Toth, State equations of the solid gas interface layer, *Acta Chim. Acad. Sci. Hung.*, 69 (1971) 311–317.
- [76] M.M. Dubinin, The potential theory of adsorption of gases and vapors for adsorbents with energetically nonuniform surfaces, *Chem. Rev.*, 60 (1960) 235–241.